Radiology Case Reports 16 (2021) 2962–2968

Available online at www.sciencedirect.com

ScienceDirect

journal homepage: www.elsevier.com/locate/radcr

Case report

MRI and CT features of a malignant myoepithelioma of the scrotum: A case report and literature review ☆,☆☆

Takayoshi Shinya, M.D. Ph.D.[a,b,*], *Yuichi Kojima, MD*[a], *Yasumasa Monobe, MD, PhD*[c], *Hideyo Fujiwara, MD*[c], *Shinya Uehara, MD, PhD*[d], *Katsuya Kato, MD, PhD*[a]

[a] *Department of Diagnostic and Therapeutic Radiology, Kawasaki Medical School General Medical Center, Okayama, Japan*

[b] *Division of Radiology, Department of Community Medicine and Medical Science, Tokushima University Graduate School of Biomedical Sciences. 2-50-1, Kuramoto-cho, Tokushima City, Tokushima, 770-8503, Japan*

[c] *Department of Pathology, Kawasaki Medical School General Medical Center, Okayama, Japan*

[d] *Department of Urology, Kawasaki Medical School General Medical Center, Okayama, Japan*

ARTICLE INFO

Article history:
Received 11 June 2021
Revised 4 July 2021
Accepted 6 July 2021

Keywords:
Malignant myoepithelioma
Scrotum, Magnetic resonance imaging
Computed tomography
Dynamic contrast-enhanced MRI
Diffusion-weighted imaging

ABSTRACT

Malignant myoepithelioma of the scrotum is extremely rare. We report the case of a 51-year-old man with malignant myoepithelioma of the scrotum, wherein computed tomography and magnetic resonance imaging revealed a lobulated soft tissue mass with calcification, cystic component, and solid component with gradual contrast enhancement on dynamic contrast-enhanced scans. The patient presented with scrotal induration, and there was no elevation of tumor markers and no evidence of a metastatic lesion on computed tomography and magnetic resonance imaging. Histopathological examination of the resected scrotal specimen confirmed a well-circumscribed solid tumor with septa, a small area of hemorrhage, and necrosis. The subsequent diagnosis was malignant myoepithelioma of the scrotum. This case shows that scrotal malignant myoepithelioma might appear as a well-defined lobulated mass with cystic regions. We conjecture that the enhancement pattern and apparent diffusion coefficient values can be potential markers for scrotal myoepithelial tumors.

☆ Acknowledgments: This research did not receive any specific grant from funding agencies in the public, commercial, or not-for-profit sectors.

☆☆ Competing interests: None of the authors have any relevant conflict of interest or industry support related to this report.

* Corresponding author. T. Shinya.
E-mail address: midnight-2005@nifty.com (T. Shinya).

https://doi.org/10.1016/j.radcr.2021.07.013

Introduction

Myoepithelial tumors (MTs) usually occur in the salivary glands and skin and occasionally in the soft tissues [1,2]. According to the World Health Organization classification system for soft tissue and bone tumors, myoepithelioma, also known as parachordoma, and myoepithelial carcinoma are classified as intermediate and malignant tumors of uncertain differentiation, respectively [3]. To the best of our knowledge, only 1 case of scrotal MTs with no information about the computed tomography (CT) and magnetic resonance imaging (MRI) findings [4] has been reported in the English literature.

We report here, a case of malignant MT of the scrotum and the features of the condition on CT and MRI, including diffusion-weighted (DW) imaging and dynamic contrast-enhanced (DCE)-MRI, with a review of the literature.

Case report

A 51-year-old man with a history of a gradually growing scrotal mass with pain was referred to our radiology department for further assessment. Physical examination revealed induration of the scrotum. The results of laboratory investigations, including levels of tumor markers, carcinoembryonic antigen, squamous cell carcinoma-related antigen, carbohydrate antigen 19-9, and α-fetoprotein, were within normal limits.

Unenhanced CT revealed a 39 mm × 27 mm × 23 mm lobulated and heterogeneous scrotal tumor hyperattenuated with tiny calcifications (Fig. 1A). Multiphasic enhanced CT revealed a well-defined mass with cystic regions and a solid part and septum, which showed gradual enhancement (Figs. 1B-D). Lymph node enlargement and distant metastases to other organs were not observed.

MRI revealed a 37 mm × 25 mm × 24 mm lobulated scrotal mass with no invasion into the surrounding tissues, including the testes and epididymis. The tumor mainly had a heterogeneous area of intermediate intensity with low signal intensity (SI) reticular structures on T2-weighted images (T2WIs) (Fig. 2A). Other parts of the tumor had high SI on fat-saturated T2WIs (Fig. 2B). The tumor had a markedly high SI area and a slightly high SI area compared with that of the muscle on T1-weighted images (T1WIs) (Fig. 2C). Moreover, no fat component was visible on fat-saturated T1WIs (Fig. 2D). On DCE-MRI (Fig. 2E) and late contrast-enhanced T1WI (Fig. 2F), the tumor showed gradual contrast enhancement in the intermediate and low SI regions on T2WIs, corresponding to the solid

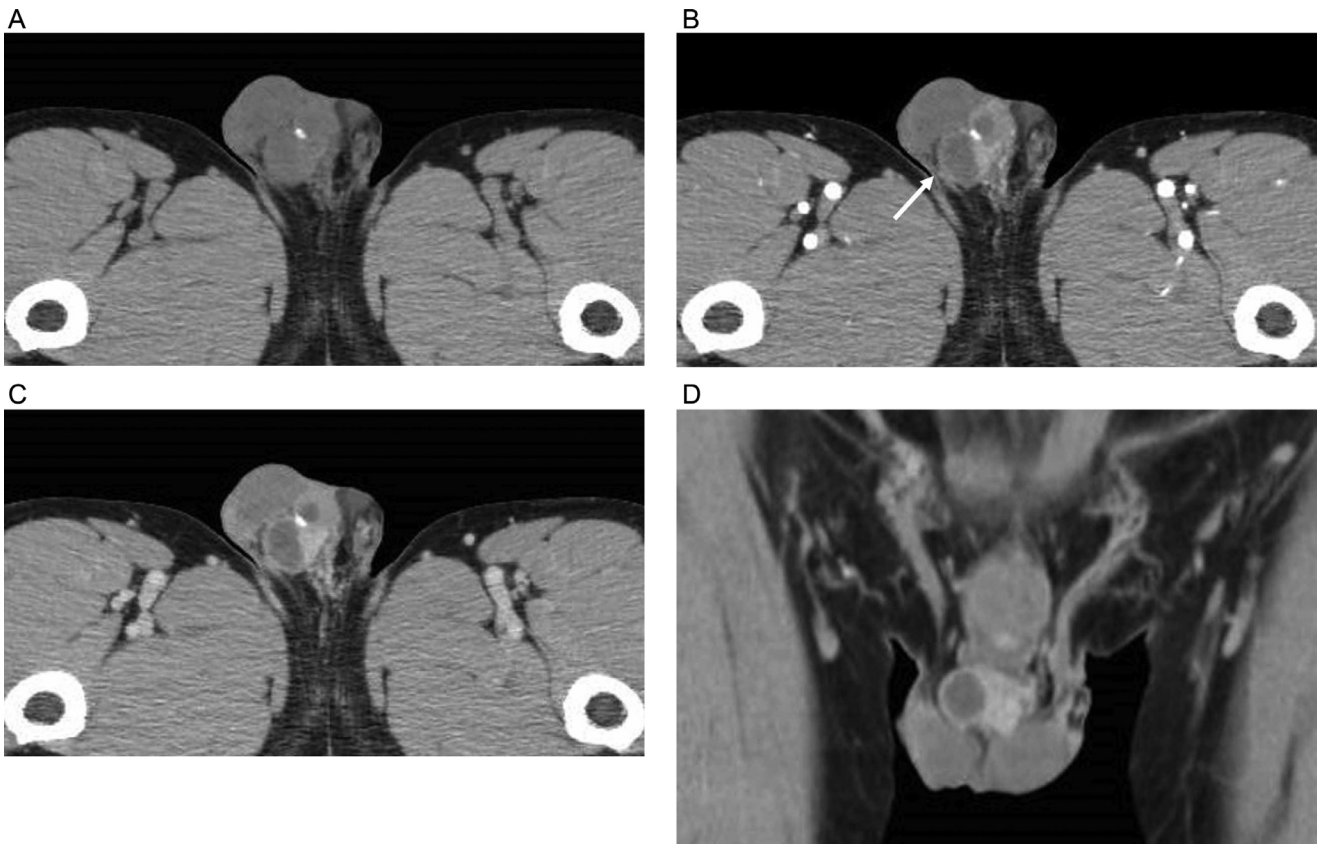

Fig. 1 – Computed tomography (CT) scans (soft tissue window).
(A) Unenhanced axial CT reveals a lobulated scrotal tumor with calcification.
(B) The tumor displays moderate heterogeneous enhancement with unenhanced cystic areas (arrow) in the early phase 30 seconds after contrast material injection (CMI) in the multiphasic enhanced CT scan.
(C, D) Enhanced CT reveals a well-defined mass with cystic regions and solid part and septum, which shows gradual enhancement in the delayed phase that is acquired at 180 seconds after CMI (c axial image; d coronal image).

Fig. 2 – Magnetic resonance imaging (MRI).
(A) Coronal T2-weighted images (T2WIs) reveal a lobulated scrotal mass with hypointense reticular structures (repetition time [TR]/effective echo time [TE], 2000/70 ms). There are no signs of infiltration to the adjacent structures (arrow).
(B) The tumor mainly has a heterogeneous intermediate intense area with an evident hyperintense area and hypointense reticular structures on coronal fat-saturated T2WIs (TE/TR, 3300/75 ms).
(C) The tumor has an isointense area compared that of the muscle and a hyperintense area on coronal T1-weighted images (T1WIs) (TE/TR, 425/13 ms).
(D) Coronal fat-saturated T1WIs reveal no fat component in the tumor (TR/TE, 7.34/3.6 ms).
(E) Coronal dynamic contrast-enhanced T1WIs reveal initial heterogeneous enhancement with progressive filling-in at the septum and solid parts (TR/TE, 7.34/3.6 ms). Pre: precontrast; 1st, 2nd, and 3rd: acquired at 35, 60, and 80 seconds after contrast material injection (CMI).
(F) Late contrast-enhanced T1WIs with fat saturation acquired at 2 minutes after CMI show a more widespread heterogeneous contrast enhancement at the septum and solid parts within the tumors (TR/TE, 425/13).
(G) Diffusion-weighted images show high signal intensity in the septum and solid parts where contrast enhancement is observed (TR/TE, 5500/64.17, b-value = 700 s/mm^2).
(H) The lowest mean apparent diffusion coefficient value of the tumors is 0.61 × 10^{-3} mm^2/s (TR/TE, 5500/64.17 ms, b-value = 700 s/mm^2).

parts and septum within the tumor. These areas had a slightly increased SI region on DW-MRI (Fig. 2G) and restriction of diffusion on apparent diffusion coefficient (ADC) maps (Fig. 2H). However, no contrast enhancement was observed in the cystic parts of the high SI regions on T2WIs, which corresponded to cystic change and myxoid degeneration with partially hemorrhagic necrosis, and the high SI region on T1WI corresponded to the hemorrhagic area.

Various preoperative differential diagnoses of benign and malignant conditions such as myxoma, degenerated

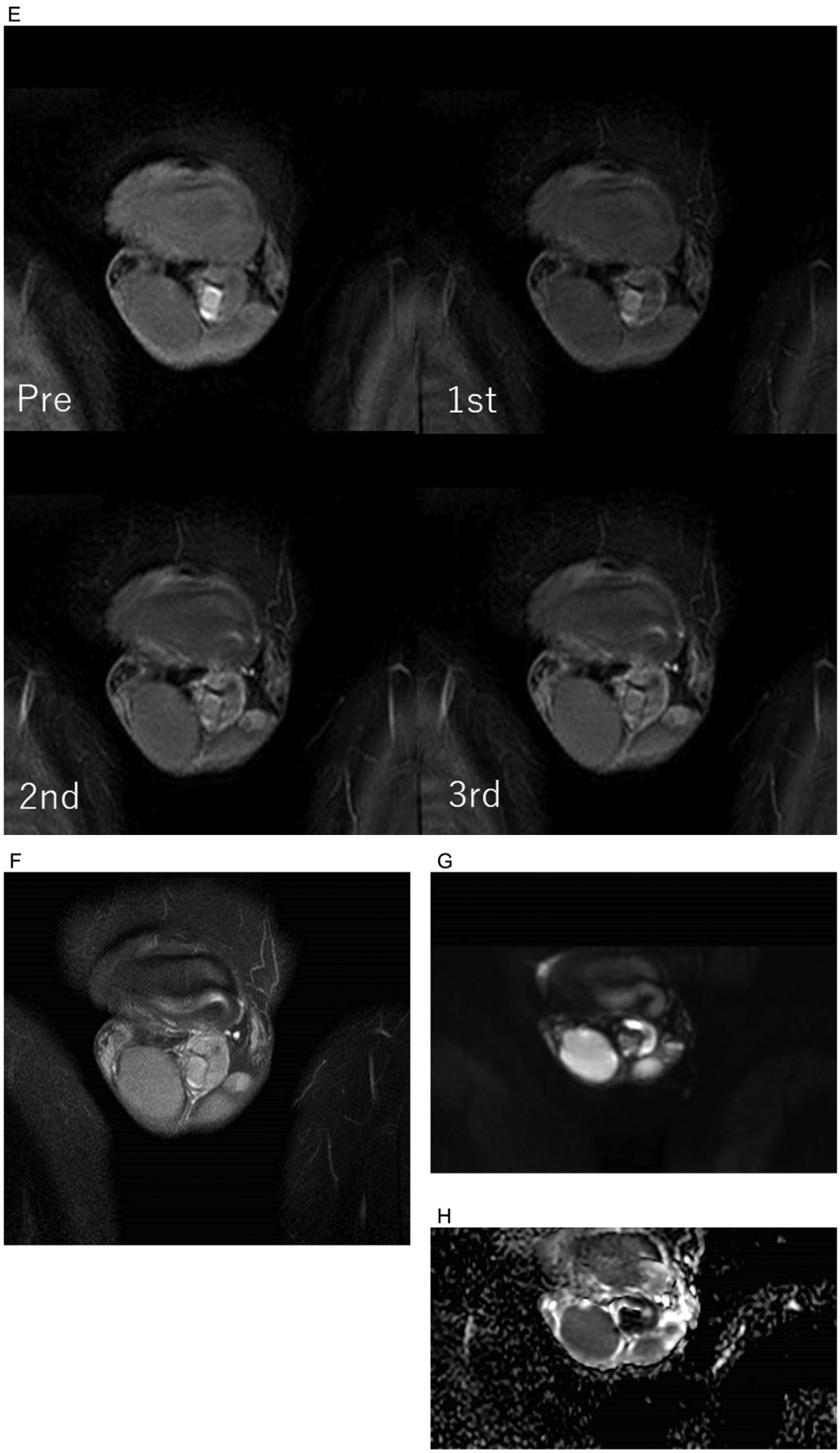

Fig. 2 – Continued

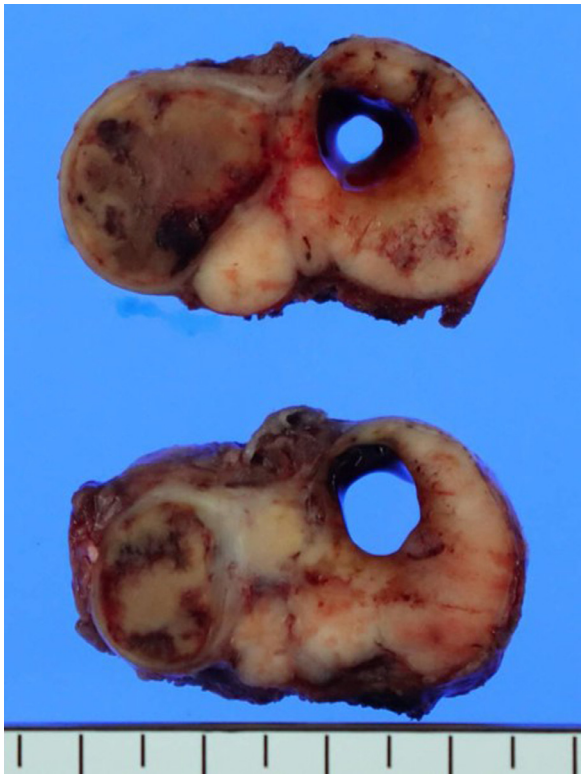

Fig. 3 – Image of the cut surface of the scrotal tumor. The cut surface of the mass shows multiple yellowish-white tumors with hemorrhage and necrosis.

leiomyoma, malignant soft tissue sarcoma, malignant peripheral nerve sheath tumor, and even metastatic carcinoma, based on nonspecific CT and MRI features of the sacral soft tissue mass, were considered. However, accurately distinguishing these lesions based on CT and MRI findings was challenging.

The tumor was excised through the scrotal approach. The tumor mass was not attached to the surrounding tissue or testicle. It had a clear margin that could be completely dissected. On the cut section, the tumor was 38 mm × 30 mm × 22 mm in size, well-defined, lobulated, yellowish-white, and firm with hemorrhage and necrotic change, which originated from the subcutaneous soft tissue (Fig. 3).

Microscopically, most tumor cells comprised round atypical cells with prominent nuclei with mitoses arranged in nests. In addition, fibrous bundles and mucinous stroma were also present (Figs. 4A and B). The tumor did not infiltrate into the surrounding tissue. Immunohistochemical analysis revealed that the tumor cells were positive for vimentin, calponin, CD10, CD99 (MIC2), and p63 and focally positive for epithelial membrane antigen, BCL2, cytokeratin (CK) CAM5.2, and Ki-67 antigen. The tumor cells were not immunoreactive for α-smooth muscle actin, desmin, α-inhibin, glial fibrillary acidic protein, CD34, CD56, CK AE1/AE3, common leukocyte antigen, S-100 protein, calretinin, and D2-40. These pathological findings led to the diagnosis of a malignant myoepithelioma (MM) of the soft tissue.

Discussion

Soft tissue MTs are rare, and the skin and salivary gland, especially the parotid glands, are the most reported sites of MTs [5–7]. Although extremely rare, the scrotum can be a primary site of MTs [1]. Although most MTs follow a benign clinical course, malignant cases exist; however, such cases are extremely rare. The incidence is not accurately known because of its rarity.

Imaging characteristics of MTs in soft tissues have not been well-described in the English literature, possibly due to their low incidence [1,5]. Several papers have reported myoepithelioma and MM in soft tissues that were evaluated on CT and MRI [1,2,5,7,8]. In these papers, the soft tissue MTs were relatively well-defined lobulated masses with moderate heterogeneous enhancement on contrast-enhanced CT. In studies that evaluated these tumors on MR imaging, the masses commonly exhibited low to intermediate intensity with high SI corresponding to the hemorrhagic areas on T1WIs and heterogeneous high intensity with internal septa of low SI on T2WIs. The masses had well-circumscribed cystic regions in the tumors on all sequences [5]. Therefore, there is no specific imaging characteristic for the differential diagnosis of MT, and there is an overlap between the benign and malignant presentation of these tumors, making it impossible to differentiate them using imaging alone. Hence, a biopsy is necessary [2]. There are no reports of MR images for sacral MTs. Moreover, no previous case about the findings on DW-MRI and DCE-MRI in patients with soft tissue MMs has been reported in the English literature. Thus, the detailed enhancement patterns of soft tissue MMs and typical ADC values remain unclear.

DCE-MRI after a bolus injection of a contrast medium is clinically used to evaluate the vascularity of the lesion. Malignant tumors usually demonstrate a gradual enhancement pattern characterized by early enhancement, and the peak contrast in malignant tumors is commonly achieved within 120 seconds in salivary gland tumors [9–11]. In a patient with epithelioid myoepithelioma of the accessory parotid gland, the time-SI curve generated from a DCE-MRI study displayed a gradual enhancement pattern [12]. In contrast, the tumor demonstrated rapid and gradual enhancement and a contrast peak in less than 120 seconds on DCE-MRI in a patient with MM of a submandibular salivary gland [9]. In addition, the dynamic enhancement curve in patients with tibial MM showed early wash-in and early wash-out; this pattern is common in both malignant tumors and aggressive lesions such as giant cell tumors of the bone, on DCE-MR images [13]. In the present case report, the sacral MM showed gradual and heterogeneous contrast enhancement in regions corresponding to the solid parts and septum within the tumor. Although the enhancement pattern of soft tissue MTs on DCE-MRI has not been fully investigated, it can be a potential characteristic for distinguishing between benign and malignant soft tissue MTs.

DW-MRI is an unenhanced functional MRI evaluation based on the diffusion motion of water molecules. In general, DW-MRI can delineate malignant lesions as a hyperintense area with excellent tissue contrast, and cases with low SI on DW-MRI can be considered as benign lesions [14–16]. A few previous papers have reported the DW-MRI feature and ADC

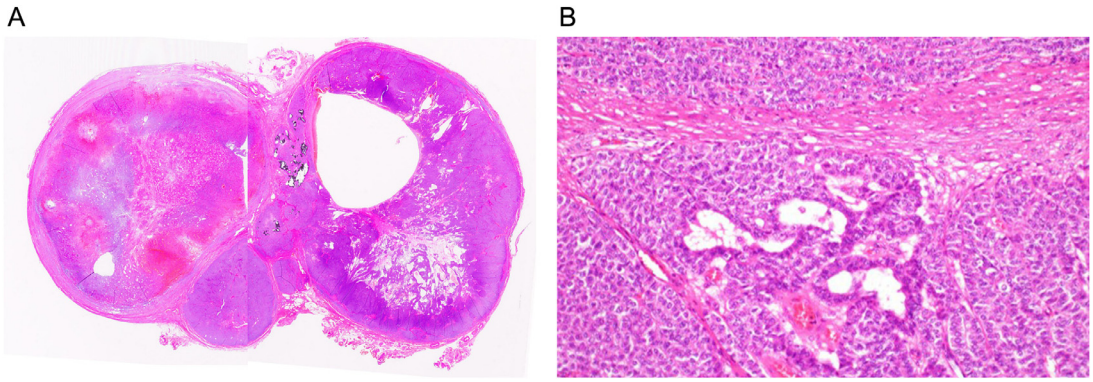

Fig. 4 – Histopathological findings of the surgical specimen.
(A) A macroscopic view of the specimen showing a lobulated tumor with hemorrhagic necrosis and cystic changes.
(B) Microscopically, the round-shaped atypical cells with prominent nuclei with mitoses are arranged in nests. The fibrous bundles and mucinous stroma are also present (hematoxylin and eosin stain; original magnification, × 200).

value of MTs [5,9,13]. Linghong Guo *et al.* reported myoepithelioma of the abdominal wall with moderately restricted diffusion [5]. In contrast, DW-MRIs showed hyperintensity, and the ADC map showed hypointensity in myoepithelial carcinoma of the tibia [13]. In a previous report, the myoepithelial carcinoma of the salivary gland had a mean ADC value of 1.35×10^{-3} mm^2/s, because of which the tumor was classified as malignant [9]. The present case showed high SI on DW-MRIs for MM with an ADC value of 0.607×10^{-3} mm^2/s. These results suggest that DW-MRIs and ADC values can be potentially useful for differentiating benign from malignant MTs, and this needs to be assessed in further investigations.

In conclusion, sacral MM presents as a well-defined lobulated mass with a cystic region and shows low to intermediate SI, with high SI corresponding to the hemorrhagic areas on T1WIs and heterogeneous high SI with internal septa of low SI on T2WIs, gradual enhancement on DCE-MRI, and high SI regions on DW-MRI with low ADC values. Although the enhancement pattern of MMs on DCE-MRI and the diagnostic efficiency of the ADC value have not been fully investigated, these can be potential markers in distinguishing benign from malignant MTs. Therefore, it is critical to consider the possibility of sacral MM when examining sacral cystic tumors with high SI on DW-MRI with an enhanced component on DCE-MRI.

Patient consent

This study does not require institutional review board approval. Informed consent was obtained for the case report to be published.

Supplementary materials

Supplementary material associated with this article can be found, in the online version, at doi:10.1016/j.radcr.2021.07.013.

REFERENCES

[1] Harada O, Ota H, Nakayama J. Malignant myoepithelioma (myoepithelial carcinoma) of soft tissue. Pathol Int 2005;55(8):510–13. doi:10.1111/j.1440-1827.2005.01861.x.
[2] Trevino M, Moorthy C, Kafchinski L, Bustamante D. Foot plantar soft tissue malignant myoepithelioma tumor: case report and review of the literature. Clin Imaging 2020;61:90–4 DOI. doi:10.1016/j.clinimag.2019.11.014.
[3] Sbaraglia M, Bellan E, Dei Tos AP. The 2020 WHO Classification of soft tissue tumours: news and perspectives. Pathologica 2020;113(2):70–84 10.32074/1591-951×-213. Online ahead of print.
[4] Flucke U, Palmedo G, Blankenhorn N, Slootweg PJ, Kutzner H, Mentzel T. EWSR1 gene rearrangement occurs in a subset of cutaneous myoepithelial tumors: a study of 18 cases. Mod Pathol 2011;24(11):1444–50. doi:10.1038/modpathol.2011.108.
[5] Guo L, Zhou F, Zhang N, Dai H, Zeng X, Gong H. Myoepithelioma of the lateral abdominal wall: a case report. Medicine 2018;97(27):e11209. doi:10.1097/MD.0000000000011209.
[6] Ellis GL, Auclair PL. Tumors of the salivary gland, atlas of tumor pathology, 3rd series, fascicle 17, pathology. Washington, DC: Armed Forces Institute; 1996.
[7] Pilavaki M, Givissis P, Tzarou V, Palladas P, Pournaras J. Soft-tissue myoepithelioma of the hypothenar region: a case report. J Hand Surg Am 2007;32(5):674–6. doi:10.1016/j.jhsa.2007.02.022.
[8] Clabeaux J, Hojnowski L, Valente A, Damron TA. Case report: parachordoma of soft tissues of the arm. Clin Orthop Relat Res 2008;466(5):1251–6. doi:10.1007/s11999-008-0125-7.
[9] Panelli Santos KCP, Matsuzaki H, Unetsubo T, Tsuyoshi S, Nagatsuka H, Asaumi JI. De novo myoepithelial carcinoma with multiple metastases arising from a submandibular salivary gland: a case report. Oncol Lett 2017;13(4):2679–83. doi:10.3892/ol.2017.5783.
[10] Hisatomi M, Asaumi J, Yanagi Y, Unetsubo T, Maki Y, Murakami J, et al. Diagnostic value of dynamic contrast-enhanced MRI in the salivary gland tumors. Oral Oncol 2007;43(9):940–7. doi:10.1016/j.oraloncology.2006.11.009.

[11] Yabuuchi H, Fukuya T, Tajima T, Hachitanda Y, Tomita K, Koga M. Salivary gland tumors: diagnostic value of gadolinium-enhanced dynamic MR imaging with histopathologic correlation. Radiology 2003;226(2):345–54. doi:10.1148/radiol.2262011486.
[12] Iguchi H, Yamada K, Yamane H, Hashimoto S. Epithelioid myoepithelioma of the accessory parotid gland: pathological and magnetic resonance imaging findings. Case Rep Oncol. 2014;7(2):310–15. doi:10.1159/000363099.
[13] Lin CH, Wu KY, Chen CKH, Li CF, Hsieh TJ. Myoepithelial carcinoma of tibia mimic giant cell tumor: a case report with emphasis on MR features. Skeletal Radiol 2019;48(10):1637–41. doi:10.1007/s00256-019-03198-w.
[14] Subhawong TK, Jacobs MA, Fayad LM. Insights into quantitative diffusion-weighted MRI for musculoskeletal tumor imaging. AJR Am J Roentgenol 2014;203(3):560–72. doi:10.2214/AJR.13.12165.
[15] Liu LP, Cui LB, Zhang XX, Cao J, Chang N, Tang X, et al. Diagnostic performance of diffusion-weighted magnetic resonance imaging in bone malignancy: evidence from a meta-analysis. Medicine 2015;94(45):e1998. doi:10.1097/MD.0000000000001998.
[16] Ahlawat S, Khandheria P, Subhawong TK, Fayad LM. Differentiation of benign and malignant skeletal lesions with quantitative diffusion weighted MRI at 3T. Eur J Radiol 2015;84(6):1091–7. doi:10.1016/j.ejrad.2015.02.019.